High Temperature NPSH and Its Application for a Feedwater System*

Jun MANABE** and Kazuyoshi MIYAGAWA**

Eight hundred MWe class PWR turbine-generators operated smoothly and continuously at sudden load reduction from full load to house load, maintaining NPSH of the feedwater booster pumps through transition even though the available NPSH never exceeded zero. NPSH of the pump at 151.3°C, at which the available NPSH was minimal during transition, was evaluated as a slightly negative value, in spite of a positive value at room temperature, applying both the Ruggeri-Moore method extended to the negative area on condition of gas venting out of the system, using data of both room temperature and 95°C of a model pump facility, and another restriction by gas presence at the impeller inlet. The above evaluated high temperature NPSH demonstrated successful operation of the units equipped with a low static suction head yielding zero available NPSH during transition, resulting in alteration of the design criteria of the feedwater system and thereby contributing to possible cost reduction.

Key Words: NPSH, Cavitation, Thermal Effect, Feedwater Booster Pump, Load Reduction, Feedwater Storage Tank

1. Introduction

Two similarly designed second generation 800 MWe class units maintained smooth operation during a sudden load reduction test in trial operations in the 1970s, followed by neither loss of the feedwater booster pump head nor tripping of the feedwater pump by interlock. Such information suggests that the NPSH of feedwater booster pumps was maintained through the transitions.

Simulation of these units showed that available NPSH rapidly reduced soon after the load reduction to a minimum value of −1 m at 240 sec revealing depressed boiling gas generated only in the FWBP casing, which was sufficiently small to be vented, resulting in saturation of the feedwater at the impeller and perhaps, slightly in the gas phase, only maintaining zero available NPSH.

Therefore, problems remain as to why zero available NPSH or a saturated condition was sufficient for feedwater booster pumps to maintain their heads in these units.

Required NPSH adopted by industry is the measured value in room temperature conditions and air saturated industrial water because of conservative designs and the difficulty of measurement at high temperature. High temperature required NPSH was evaluated by the Ruggeri-Moore method taking advantage of the thermal effect of cavitation, and extended to the negative area on condition of gas venting out of the system, maintaining both the residual feedwater in the saturation condition and the same flow pattern in the blade passage as in the positive pressure condition.

The presented integrated configuration of high temperature required NPSH using both the Ruggeri-Moore method and gas presence at the impeller inlet provides a solution to the problems and alters the design criteria of the feedwater system thereby contributing to possible cost reduction by allowing for a ground-level smaller capacity DTR-tank, and smaller horizontal type higher rotative speed pump.

Symbols:

FWBP : feedwater booster pump

FWP : feedwater pump

DTR-tank : deaerator and feedwater storage tank

P_d : DTR-tank pressure

H : static head from DTR-tank water level to FWBP impeller

ΔP : total pressure drop from DTR-tank to FWBP impeller

P_{sat} : saturation pressure corresponding to impeller inlet feedwater temperature

* Received 30th September, 2005 (No. 05-4189)

** Mitsubishi Heavy Industries, Ltd., 2–1–1 Shinhama, Arai-cho, Takasago, Hyogo 676–8686, Japan.
E-mail: jun_manabe@mhi.co.jp; kazuyoshi_miyagawa@mhi.co.jp

$NPSH_{av}$: available NPSH
$NPSH_{req}$: required NPSH
$NPSH_0$: NPSH yielding no head down in condition of room temperature and saturation air
γ : specific weight of feedwater at impeller inlet [kg/m^3]
ϕ : pump head
ϕ_{NC} : pump head with sufficient NPSH
h_v : vapor pressure [m]
ρ : density [kg/m^3]
L : latent heat [J/kg]
cp_l : specific heat of liquid [J/(kg·K)]
T : temperature of free-stream liquid [K]
V_l : liquid volume concerning evaporation [m^3]
V_v : gas volume concerning evaporation [m^3]
α : thermal diffusivity [m^2/hr]
U : representative velocity [m/s]
D : representative length [m]
Δx : cavity length [m]
Subscript
l : liquid
v : vapor
ref : reference
pred : prediction

2. Turbine-Generator Sudden Load Reduction and NPSH of FWBP

2.1 Construction of feedwater system

The feedwater system of the PWR turbine unit, shown in Fig. 1, consists of high and low pressure feedwater heaters, a DTR-tank, all of which are heated by turbine extraction steam, FWBPs and FWPs. The DTR-tank level is controlled by the condensate control valve. The DTR-tank is designed to have a capacity corresponding to 4 – 5 minutes of feedwater and to have a 12 – 25 m static head for the FWBP impeller. FWPs are interlocked to trip themselves for complete head loss of FWBPs to prevent cavitation.

The NPSH studied here is a suction head which yields complete head loss rather than 3% head reduction, although a suction head yielding more than half of head reduction was used because of the difficulty of the testing conditions yielding zero head.

2.2 NPSH of FWBP

More than half of the rated feedwater is continuously requested for about 3 – 4 minutes after turbine-generator load reduction for reactor cooling. DTR-tank pressure and its saturation condition temperature, about 1 MPa and 180°C, respectively, at full load or initial transition value, begin to reduce both by stoppage of its heating steam from turbine extraction, derived from a turbine casing pressure decrease, and by the continuation of colder condensate flow-in from the condenser to maintain the DTR-tank level via low pressure feedwater heaters, for which the heating

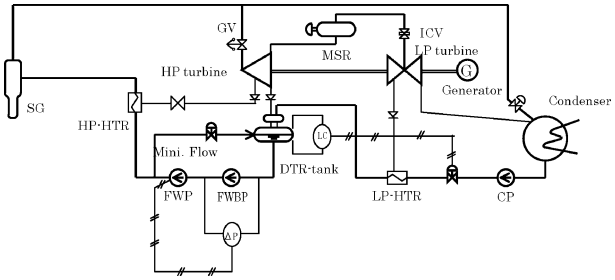

Fig. 1 Construction of PWR turbine unit system

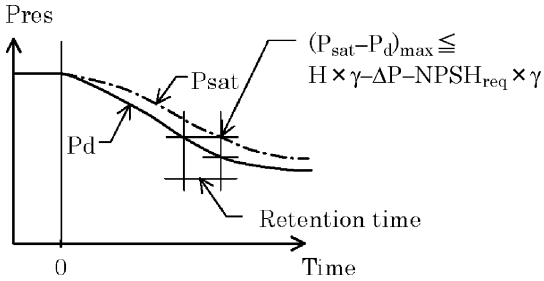

Fig. 2 NPSH of FWBP after sudden load reduction

extraction steam has also failed[1].

$$NPSH_{av} = (P_d - \Delta P)/\gamma + H - P_{sat}/\gamma \quad (1)$$

Available NPSH of FWBP shown in Eq. (1) begins to reduce at sudden load reduction according to the reduction of both pressure and associated saturated temperature of the DTR-tank because the feedwater temperature at the FWBP impeller inlet becomes higher than that of the DTR-tank derived from the retention time of the feedwater through piping and pump casing from tank to pump impeller, which means the Pd-P_{sat} becomes a negative value (Fig. 2). $NPSH_{av}$ is designed to maintain larger than $NPSH_{req}$ through transition (Eq. (2)).

$$NPSH_{av} \geq NPSH_{req} \quad (2)$$

3. Available NPSH in Actual Unit and Residual Problem

3.1 Experience of actual units

Two similarly designed second generation 800 MWe class units A-1 and A-2, having a DTR-tank situated at ground level with a static head of 11.7 m for the impeller of vertical type FWBP, with no control other than DTR-tank level control and FWP minimum flow control (common to FWP and FWBP), maintained smooth operation during a sudden load reduction test in trial operations in the 1970s, with neither loss of the FWBP head nor tripping of the FWP by interlock. This information suggests that the NPSH of FWBPs was maintained through the transitions.

In contrast, another similarly designed unit B, which differs slightly from units A-1 and A-2 in the piping arrangement between the DTR-tank and FWBP, where the

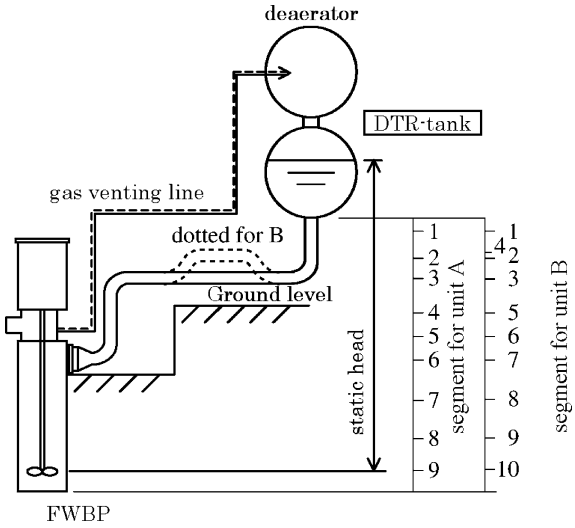

Fig. 3 Arrangement of DTR-tank, FWBP and segment for simulation

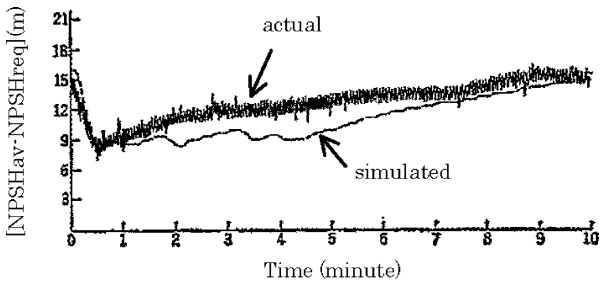

Fig. 4 Verification of simulation

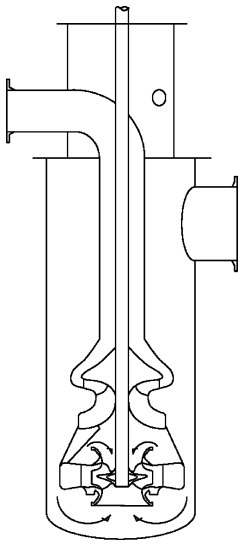

Fig. 5 Construction of FWBP

pipe was arranged upwards and then downwards forming a possible gas pocket and which was considerably longer, lost its $2 \times 50\%$ capacity FWPs' function because of FWBP head loss and tipping of FWPs by interlock, although the additional start of another $1 \times 50\%$ stand-by FWP did maintain the feedwater requirement. The arrangement of the DTR-tank, FWBP, and piping for units A and B is shown in Fig. 3.

3.2 Simulation of $NPSH_{av}$ in actual units

Available NPSH for FWBP was evaluated by a simulation, modeling the system ranging from DTR-tank to FWBP via feedwater piping to the pump casing with the piping and the pump casing divided into several segments with volume and elevation given as shown in Fig. 3. The method was to calculate the enthalpy, pressure and temperature of each element (corresponding to the segment) by thermal and mass balance between the elements and finally to calculate $NPSH_{av}$ and quality of feedwater at each element, by a simulation program using node-link networks of thermal-fluid elements named "PRANET"[2].

The accuracy of the program had been verified in case of another actual unit[3], designed to maintain sufficient $NPSH_{av}$ through transition, using actually measured data of feedwater flow, minimum flow of FWP, pressure and water level of DTR-tank, by demonstrating equivalency of the simulated $NPSH_{av}$ to the actual one derived from the measured feedwater pressure and temperature at the impeller inlet. The simulated and actual ones of the difference of $(NPSH_{av} - NPSH_{req})$ is shown in Fig. 4, using for both cases a same value of the $NPSH_{req}$ of 7.5 m measured in room temperature and saturation air. Simulation of $NPSH_{av}$ in unit A and B were also conducted as was for above.

The construction of FWBP in Fig. 5 is for both A and B unit, with two stage impellers and double flow suction for the first stage to reduce $NPSH_{req}$.

Simulation of unit A, presented in Fig. 6 (a) (measured data), 6 (b) (the simulated impeller inlet feedwater pressure, saturation pressure corresponding to simulated impeller inlet feedwater temperature of P_{sat} and $NPSH_{av}$), 6 (c) (steam quality in suction pipe and FWBP casing), showed that $NPSH_{av}$ rapidly reduced soon after the load reduction to a minimum value of -1 m at 240 sec, then recovered, attributable to interlocked opening of the FWP minimum flow line resulting in a shorter retention time. The steam quality distribution of the suction line, divided into 9 segments (Fig. 3), showed depressed boiling gas generated at 240 sec only in the FWBP casing, segments 7, 8, 9, which were calculated to be about 2.0 t/h and were sufficiently small compared to an allowable gas amount of about 3.0 t/h (corresponding to generating gas of -1.5 m of $NPSH_{av}$) by pressure difference in the drive, which was vented by 80 A diameter piping from the FWBP casing top to the DTR-tank gas area, resulting in saturation of the feedwater at the impeller and perhaps slightly in a gas phase.

However, simulation for unit B, presented in Fig. 7 (a) (measured data), 7 (b) (the simulated pump inlet feedwater pressure, P_{sat} and $NPSH_{av}$), 7 (c) (steam quality in suction pipe and FWBP casing), with its suction line divided

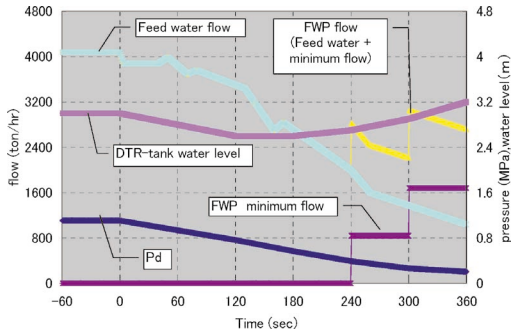

(a) Simulation of A unit – 1/3

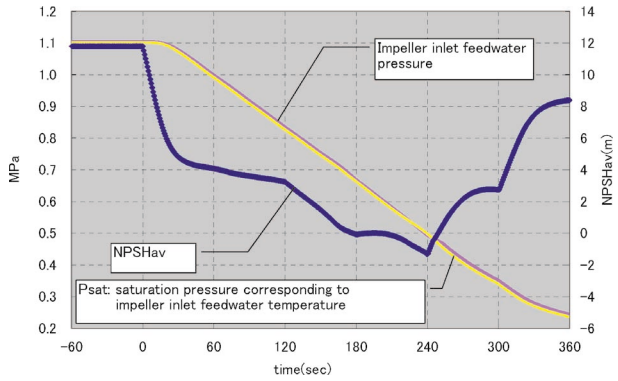

(b) Simulation of A unit – 2/3

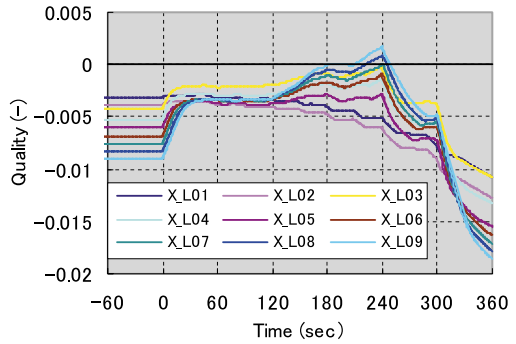

(c) Simulation of A unit – 3/3

Fig. 6 Simulation of A unit

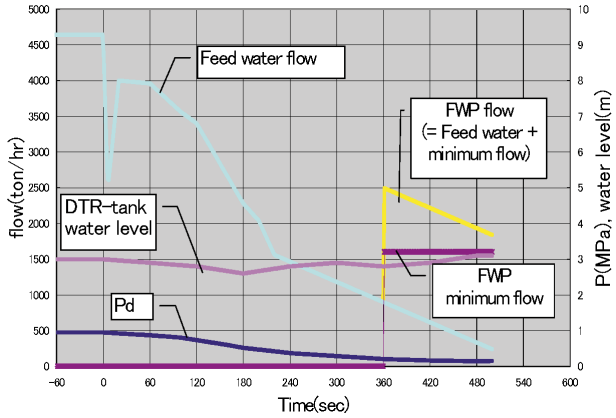

(a) Simulation of B unit – 1/3

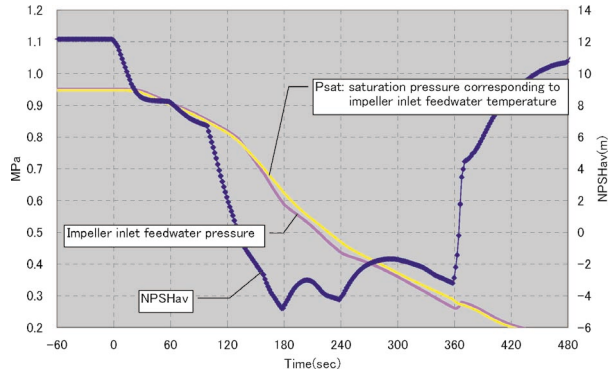

(b) Simulation of B unit – 2/3

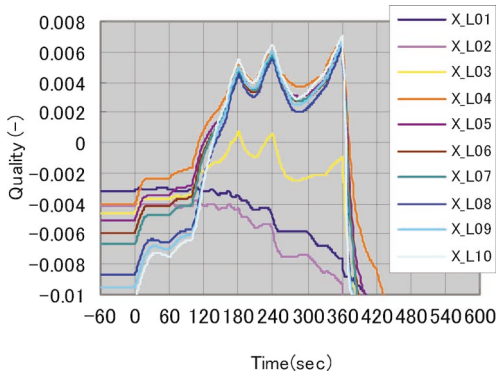

(c) Simulation of B unit – 3/3

Fig. 7 Simulation of B unit

into 10 segments, showed that $NPSH_{av}$ rapidly reduced to about −5 m, indicating the gas quality was positive, generating depressed boiling, throughout the suction line from the FWBP casing to the horizontal piping containing the pocket shaped area (segment 4), except for the descending line below the DTR-tank. The generated gas in the FWBP casing of about 7.0 t/h was larger than the venting capacity. Furthermore, the generated gas in the pocket shaped piping, which was not equipped with a venting line, stagnated to plug the piping. Both resulted in FWBP head loss.

3.3 Problems to be solved

Analyses stated above demonstrated that unit A-1 and A-2 could only maintain zero $NPSH_{av}$ or saturated water with a small volume of gas, but unit B could neither maintain sufficient $NPSH_{av}$ nor transport feedwater because of plugged gas in the piping.

Therefore, the problem remains as to why zero $NPSH_{av}$ or a saturated condition is sufficient for FWBPs to maintain their head in units A-1 and A-2.

4. High Temperature NPSH

$NPSH_{req}$ adopted by industry is the measured value in conditions of room temperature and air saturated industrial water despite the possibility of decrease at higher temperature, because of conservative designs and the difficulty of measurement at high temperature, whereas the actual operation conditions, for example, of feedwater in FWBP through transition ranges from initial 180°C, 100% flow to stabilized 120°C, 25% of pump minimum flow, deaerated

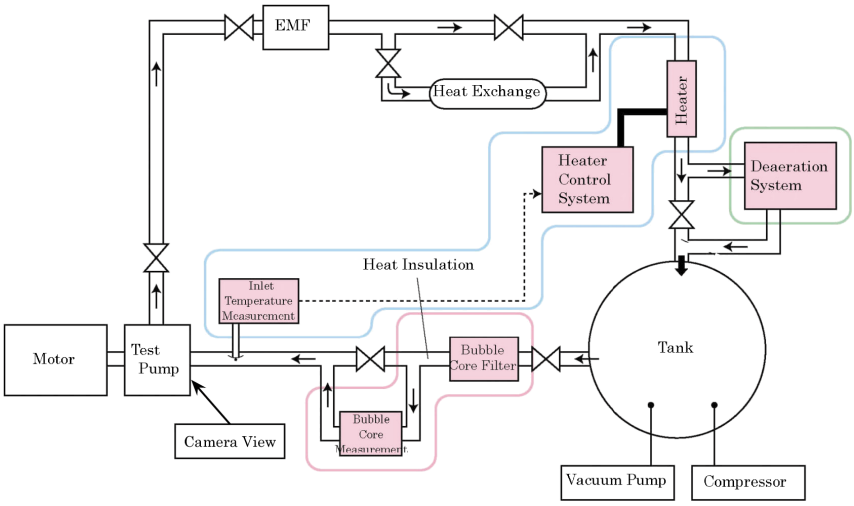

Fig. 8 Pump test facility

to 5 ppb.

Methods for predicting higher temperature $NPSH_{req}$ have been reported by Ruggeri, Stepanof and others. The Ruggeri-Moore[4] method taking advantage of the thermal effect of cavitation was utilized here, using experimental data of the modeled impeller at room temperature and 95°C.

4.1 Experiment

4.1.1 Experimental conditions Pump head alteration and others were measured along with the reduction of $NPSH_{av}$ by reducing the pump inlet pressure using a model pump facility equipped with a deaerator, pressure controlled feedwater tank, heat exchanger for process temperature control, electro-magnetic flow element, thermocouples, filter for core bubble, and sight flow window as shown in Fig. 8.

Figure 10 (b) shows the model pump impeller with a 0.244 8 m outlet diameter (2 460 rpm, 74.13 L/s flow rate). This model's ratio was 0.39 of the actual centrifugal impeller (885 rpm, 0.623 m diameter, 439.57 L/s flow rate).

The water conditions of the tested process were room temperature with saturated air, room temperature deaerated to nearly 100 ppb, high temperature of about 95°C deaerated to nearly 30 ppb, each with varying flow amounts from 40%, 60%, 80%, 100%, and over the rated point of 130%, respectively.

4.1.2 Results of experiment Both deaeration and temperature increase contributed to reducing $NPSH_{req}$, which was defined as yielding 3% head down, by 0.08 with deaeration and by 0.04 with temperature rise to 95°C, respectively at rated flow, shown in Fig. 9 (a) as the ratio to $NPSH_0$ of 5.0 m which does not yield head down in condition at room temperature and in saturated air.

There was no interference in scatter band of 99.5% reliability for both room temperature with deaerated and

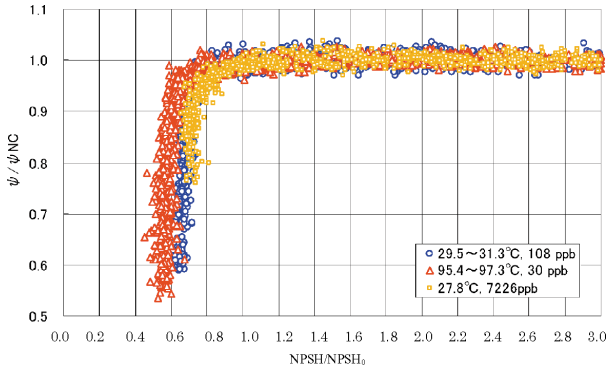

(a) NPSH of rated flow at room temperature with and without deaeration, and 95°C

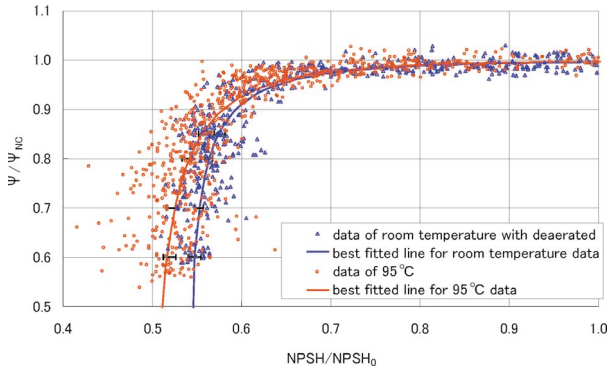

(b) Scatter band of 99.5% reliability

Fig. 9 Results of experiment of temperature dependency and deaeration effect for $NPSH_{req}$

95°C of the above test run in the range of $\phi/\phi_{NC} = 0.6$–0.85, explaining the temperature dependency of $NPSH_{req}$, as shown in Fig. 9 (b).

Visualized data for a moment of each condition with nearly the same $NPSH_{av}$ exhibited cavity air from upper stream piping in the case of room temperature with saturated air, cavity gas of water generated on the surface

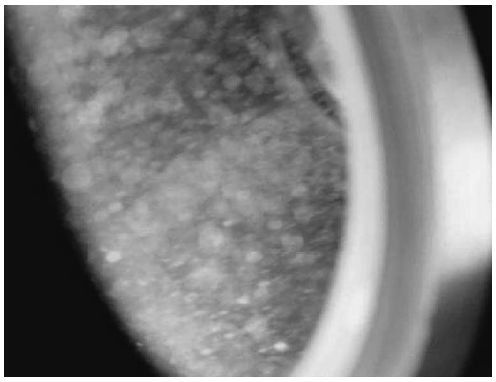

(a) Visualized data at room temperature with saturated air, $NPSH_{av} = 7.93$ m, rated flow

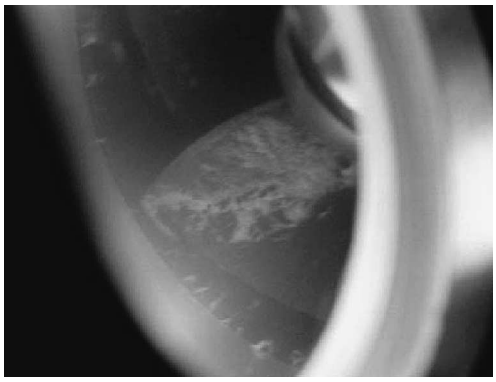

(c) Cavitation on impeller at 95°C deaerated to 33 ppb, $NPSH_{av} = 8.06$ m, rated flow

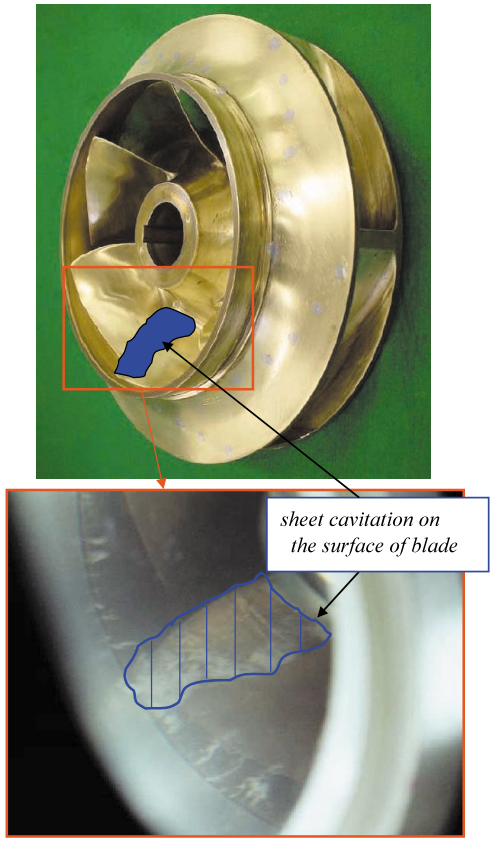

(b) Model impeller and cavitation on impeller at room temperature deaerated to 134 ppb, $NPSH_{av} = 7.93$ m, rated flow

Fig. 10 Model Impeller and visualized data for a moment in various conditions with nearly the same $NPSH_{av}$

of impeller in the case of both room temperature deaerated and 95°C deaerated, shown in Fig. 10 (a) – (c), respectively.

4.2 Prediction of high temperature $NPSH_{req}$

Higher temperature $NPSH_{req}$ derived from gas occupation and plugging in the passage between blades by yielding gas on the blade surface was evaluated by applying the Ruggeri-Moore method using data of the above test, and summarized as follows.

A certain amount of bulk water adjacent to the cavity is deprived of its heat by latent heat for the yielding cavity. Reduction of vapor pressure Δh_v of the bulk water corresponding to temperature reduction is shown in Eq. (3).

$$\Delta h_v = \frac{1}{g}\left(\frac{\rho_v}{\rho_l}\right)^2\left(\frac{L^2}{c_{pl}T}\right)\left(\frac{V_v}{V_l}\right) \tag{3}$$

The gas to liquid volume ratio of V_v/V_l, which concerns evaporation, is evaluated from experimental equation 4 (Eq. (4)), showing the relation between the two conditions, because the ratio could not be measured directly.

$$\left(\frac{V_v}{V_l}\right)_{pred} = \left(\frac{V_v}{V_l}\right)_{ref}\left(\frac{\alpha_{ref}}{\alpha}\right)^{1.0}\left(\frac{U_0}{U_{0,ref}}\right)^{0.8} \times\left(\frac{D}{D_{ref}}\right)^{0.2}\left(\frac{\Delta x/D}{(\Delta x/D)_{ref}}\right)^{0.3} \quad (4)$$

$(\Delta h_v)_{\mathrm{ref}}$ and $(\Delta h_v)_{\mathrm{pred}}$ are calculated for room temperature and 95°C respectively, by the heat relation in Eq. (5) for an assumed $(V_v/V_l)_{\mathrm{ref}}$ and corresponding $(V_v/V_l)_{\mathrm{pred}}$ derived from Eq. (4).

$$\Delta h_v = \frac{\rho_v}{\rho_l}\frac{V_v}{V_l}\frac{L}{c_{pl}}\left(\frac{dh_v}{dT}\right) \quad (5)$$

The $(V_v/V_l)_{\mathrm{ref}}$ which gives equivalency between the calculated and experimented results of $[(\Delta h_v)_{\mathrm{ref}} - (\Delta h_v)_{\mathrm{pred}}]$ leads, by Eq. (4), to $(V_v/V_l)_{\mathrm{pred}}$ for any temperature and rotative speed, as long as both flow coefficient and head coefficient are equivalent in the scaled pump. The $(V_v/V_l)_{\mathrm{pred}}$ yields the delta saturation pressure Δh_v or reduction of $\mathrm{NPSH_{req}}$ using Eq. (3).

Cavity length in the Eq. (4) was regarded as constant in the prediction for higher temperature NPSH because the prediction manner was to calculate the NPSH which gave both the same head coefficient and the same flow coefficient as of the referenced two temperature conditions, where the flow pattern between the impellers was identical implying the cavity length was constant through the temperature conditions from the referenced ones to the predicted.

4.3 Influence of gas presence at impeller inlet

In contrast, according to $\mathrm{NPSH_{av}}$ reduction to a negative value, the gas volume ratio to gas-water mixture at the impeller inlet increases sufficiently to affect the pump head. According to Minemura and others, increase of the ratio up to 6–7% reduces head gradually to several percent and then reduces the head rapidly to zero head within the ratio nearly 10% in case of a centrifugal pump[5]. The gas to gas-water mixture volume ratio of 10% corresponds to that in condition of −0.25 m of the $\mathrm{NPSH_{av}}$ at 151.3°C, resulting in another $\mathrm{NPSH_{req}}$.

5. Configuration of High Temperature NPSH

5.1 Extension of Ruggeri-Moore method to negative area

High temperature NPSH predicted by the Ruggeri-Moore method is the NPSH derived from gas occupation and plugging in the passage between blades by yielding gas on the blade surface, using the experimental data of two different conditions of positive pressure at the impeller inlet. The method is applicable in the area where positive pressure at the impeller inlet is assured to maintain the same flow pattern as that in the reference experiments.

The Ruggeri-Moore method may be applicable even in the area where NPSH is a negative figure by further temperature rise on condition that boiling gas at impeller inlet is vented out of the system because the residual feedwater is maintained in the saturation condition and gives the same flow pattern as that requested. Boiling gas venting capability depends not only on the amount of boiling gas, but also on feedwater velocity and arrangement of the suction piping, as well as the pressure difference in driving. The residual feedwater temperature decrease by derivation of latent heat for boiling gas is sufficiently small of about 1°C, corresponding to 0.2% quality or $\mathrm{NPSH_{req}}$ of −1 m shown in Fig. 6 (c) in the case of units A-1 and A-2, for prediction reliability of high temperature NPSH at 151.3°C, although the error will increase according to further reduction of NPSH.

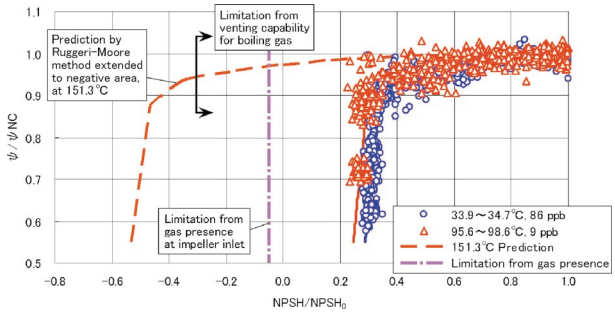

Fig. 11 Integrated high temperature NPSH configuration, 151.3°C, 40% rated flow of A units

5.2 Integrated configuration of high temperature NPSH

Integrated configuration of high temperature NPSH presented here is the combined one with the prediction of the Ruggeri-Moore method extended to the negative area on condition of gas venting and the restriction from the impeller inlet gas presence, illustrated in Fig. 11, in the condition of 151.3°C at 40% flow rate of units A-1 and A-2, for example, where $\mathrm{NPSH_{av}}$ of FWBP became minimal through the transition.

The figure shows that $\mathrm{NPSH_{req}}$ maintaining half of the rated head is larger than −0.5 $\mathrm{NPSH/NPSH_0}$ or −2.5 m with gas venting and considerably larger than −0.05 $\mathrm{NPSH/NPSH_0}$ or −0.25 m but slightly a minus without venting, respectively, but the venting capability for the impeller inlet restricts the former to larger than −0.3 $\mathrm{NPSH/NPSH_0}$ or −1.5 m for units A-1 and A-2.

The integrated configuration of high temperature NPSH is to be used only in a slightly little minus area to understand the mechanism of operation in condition of saturation or a little gas containing.

6. Conclusion

6.1 High temperature NPSH

High temperature NPSH was evaluated and presented as an integrated configuration, using both the Ruggeri-Moore method extended to the negative area on condition of gas venting out of the system, and by gas presence at

the impeller inlet without gas venting.

The presented High Temperature $NPSH_{req}$ with a slightly minus value at the temperature demonstrated the successful operation of units A-1 and A-2 maintaining zero $NPSH_{av}$ at a sudden load reduction with sufficient venting capacity.

6.2 Application for design

The integrated high temperature NPSH configuration has altered the design criteria of the feedwater system to adopt a zero value of the $NPSH_{req}$ by facilitating both sufficient venting capacity and once-through descending piping arrangement as short as possible, thereby contributing to possible cost reduction by allowing for a ground-level smaller capacity DTR-tank, and smaller horizontal type higher rotative speed pump.

Acknowledgment

The authors would like to acknowledge the advice and assistance provided by the High Temperature NPSH project team members Makoto Taniguchi, Yuji Fujii, Kimio Akazawa, Eiichi Hosomi, Koichi Inoue, Toshiki Kojima, Shinji Fukao, and Carlos Tajima.

References

(1) Araki, R., Kokubo, R., Nakagami, Y., Kawada, Y., Obara, I. and Hayami, K., Recent Technology on PWR Secondary System (Turbine Generator Plant), Mitsubishi Heavy Industries Technical Journal, (in Japanese), Vol.19, No.6 (1982), pp.80–95.

(2) Kuwabara, K. and Murata, R., Simulation Program Using Node-Link Network of Fluid Plants, Mitsubishi Heavy Industries Technical Journal, (in Japanese), Vol.22, No.6 (1985), pp.55–58.

(3) Nakagami, Y., Yoshioka, T., Sasaki, T., Manabe, J., Matsukuma, M., Taniguchi, M. and Miyawaki, T., Design and Field Operation of Advanced 900 MW Class PWR Turbine Plant, Mitsubishi Heavy Industries Technical Journal, (in Japanese), Vol.22, No.3 (1985), pp.38–45.

(4) Ruggeri, R. and Moore, R., Method for Prediction of Pump Cavitation Performance for Various Liquids, Liquid Temperatures, and Rotative Speeds, NASA TN D-5292, Lewis Research Center, Cleveland, Ohio, NASA, (1969).

(5) Minemura, K., Uchiyama, T., Shoda, S. and Egashira, K., Prediction of Air-Water Two-Phase Flow Performance of a Centrifugal Pump Based on One-Dimensional Two-Fluid Model, Journal of Fluids Engineering, ASME, Vol.120, June (1998), pp.327–334.